Published in final edited form as:
*Neurobiol Dis*. 2012 February ; 45(2): 683–691. doi:10.1016/j.nbd.2011.10.009.

# Increased efficiency of the GABAA and GABAB receptor–mediated neurotransmission in the Ts65Dn mouse model of Down syndrome

**Alexander M. Kleschevnikov**[1,2,*], **Pavel V. Belichenko**[1,2], **Jessica Gall**[2], **Lizzy George**[2], **Rachel Nosheny**[3], **Michael T. Maloney**[2], **Ahmad Salehi**[2,4], and **William C. Mobley**[1,2]

[1]Department of Neurosciences, University of California, San Diego, 9500 Gilman Drive, La Jolla, CA, 92093

[2]Department of Neurology, Stanford University Medical School, 1201 Welch Rd., Stanford, CA, 94305

[3]Molecular and Cellular Physiology, Stanford University Beckman Ctr., 259 Campus Dr., B139 Stanford, CA 94305

[4]Department of Psychiatry, VA Palo Alto Health Care System, 3801 Miranda Ave, 151Y, Palo Alto, CA 94304

## Abstract

Cognitive impairment in Down syndrome (DS) involves the hippocampus. In the Ts65Dn mouse model of DS, deficits in hippocampus-dependent learning and synaptic plasticity were linked to enhanced inhibition. However, the mechanistic basis of changes in inhibitory efficiency remains largely unexplored, and efficiency of the GABAergic synaptic neurotransmission has not yet been investigated in direct electrophysiological experiments. To investigate this important feature of neurobiology of DS, we examined synaptic and molecular properties of the GABAergic system in the dentate gyrus (DG) of adult Ts65Dn mice. Both GABAA and GABAB receptor-mediated components of evoked inhibitory postsynaptic currents (IPSCs) were significantly increased in Ts65Dn vs. control (2N) DG granule cells. These changes were unaccompanied by alterations in hippocampal levels of GABAA (α1, α2, α3, α5 and γ2) or GABAB (Gbr1a and Gbr1b) receptor subunits. Immunoreactivity for GAD65, a marker for GABAergic terminals, was also unchanged. In contrast, there was a marked change in functional parameters of GABAergic synapses. Paired stimulations showed reduced paired-pulse ratios of both GABAA and GABAB receptor-mediated IPSC components (IPSC2/IPSC1), suggesting an increase in presynaptic release of GABA. Consistent with increased gene dose, the level of the Kir3.2 subunit of potassium channels, effectors for postsynaptic GABAB receptors, was increased. This change was associated with enhanced postsynaptic GABAB/Kir3.2 signaling following application of the GABAB receptor agonist baclofen. Thus, both GABAA and GABAB receptor-mediated synaptic efficiency is increased in the Ts65Dn DG, thus likely contributing to deficient synaptic plasticity and poor learning in DS.



*Correspondence to: Alexander M. Kleschevnikov, PhD, Department of Neurosciences, University of California, San Diego, 9500 Gilman Drive, La Jolla, CA, 92093 Tel: (858) 534-1089; akleschevnikov@yahoo.com.

**Keywords**

Inhibitory system; GABAA receptor; GABAB receptor; evoked inhibitory postsynaptic currents; IPSC; potassium channels; Kir3.2 subunits; dentate gyrus; Down syndrome

## Introduction

Down syndrome (DS) is characterized by intellectual disability resulting in part from deficits in hippocampally-mediated learning and memory (Carlesimo et al., 1997; Roizen and Patterson, 2003). Mouse genetic models have provided valuable insights into the cellular and molecular mechanisms responsible for DS-related changes (Coyle et al., 1991; Reeves, 2006; Salehi et al., 2006; Moore and Roper, 2007; Salehi et al., 2007; Salehi et al., 2009; Chakrabarti et al., 2010). The Ts65Dn mouse is segmentally trisomic for chromosome 16, bearing an extra copy of ~115 genes homologous to those on human chromosome 21 (Davisson et al., 1993; Gardiner et al., 2003; Olson et al., 2007; Sturgeon and Gardiner, 2011). Accordingly, Ts65Dn mice recapitulate a number of physiological and behavioral features of DS (Holtzman et al., 1996; Siarey et al., 1997; Dierssen et al., 2001; Galdzicki and Siarey, 2003; Costa and Grybko, 2005; Hanson et al., 2007).

Previously we found that deficient synaptic plasticity in the dentate gyrus (DG) of Ts65Dn mice is associated with an imbalance of excitatory and inhibitory neurotransmission favoring the latter (Kleschevnikov et al., 2004). It was demonstrated subsequently that suppression of inhibitory neurotransmission using GABAA receptor antagonists reverses cognitive deficits of DS model mice in hippocampally-mediated memory tasks (Fernandez et al., 2007; Rueda et al., 2008). These findings powerfully motivated studies to decipher changes in inhibitory synaptic structure and function. In recent studies multiple structural and biochemical changes of the GABAergic system have been described in DS model mice (Belichenko et al., 2004; Belichenko et al., 2007; Best et al., 2007; Belichenko et al., 2009a; Belichenko et al., 2009b; Chakrabarti et al., 2010; Cramer et al., 2010). However, changes in efficiency of inhibitory neurotransmission have not yet been investigated in direct electrophysiological experiments, and the underlying cellular and molecular mechanisms of the ‘over-inhibition’ in DS remain largely undefined. Furthermore, the relative degree of changes in the GABAA vs. GABAB receptor-mediated efficiency has not been yet investigated. Such studies are essential to understanding the neurobiology of the cognitive deficits in DS, as well as for the potential development of new treatments for improving learning and memory in this developmental disorder. To explore the synaptic and cellular mechanisms of enhanced inhibitory efficiency in Ts65Dn DG, we used a combination of electrophysiological, biochemical and immunohistochemical methods.

Here we present the first direct electrophysiological evidence of enhanced efficiency of GABAergic synaptic transmission in a DS mouse model. Both GABAA and GABAB receptor-mediated synaptic responses were significantly increased in the Ts65Dn DG. This increase was accompanied by a reduction of paired-pulse ratios (PPR, IPSC2/IPSC1) of both IPSC components, suggesting an increase in presynaptic release of GABA. Furthermore, we observed an increased signaling through the postsynaptic GABAB receptors that use as effectors Kir3.2 subunit-containing inwardly-rectifying potassium channels. The enhancement in GABAB/Kir3.2 signaling was associated with an increased level of Kir3.2 protein, owing to DS-specific genetic triplication (gene *Kcnj6*). There was no evident change in the distribution of GABAergic inputs by immunohistochemistry, or in the levels of GABAA and GABAB receptor subunits by Western blot. Thus, over-inhibition in the Ts65Dn DG is likely caused by changes in the function of individual GABAergic synapses. The data raise the possibility that antagonists of both GABAA and GABAB receptors, as

well as blockers of Kir3.2 subunit–containing potassium channels, may be used to restore the excitatory/inhibitory balance and to correct cognitive deficits in people with DS.

## Materials and methods

### Animal Husbandry

Segmental trisomy 16 (Ts65Dn) mice were obtained by mating female carriers of the $17^{16}$ chromosome (B6EiC3H-a/A-Ts65Dn) with (C57BL/6JEi X C3H/HeJ)F1 (JAX #JR1875) males (Davisson et al., 1993). Ts65Dn mice are thus maintained on the B6/C3H background. To distinguish 2N from Ts65Dn mice, tail samples were used to extract genomic DNA; a quantitative polymerase chain reaction protocol developed by the Jackson Laboratory, Bar Harbor, ME (http://www.jax.org/cyto/quanpcr.html) was used to measure expression of the myxovirus resistance 1 (*Mx1*) and apolipoprotein B control (*Apob*) genes. *Mx1* is present in three copies and *Apob* in two copies in Ts65Dn mice. The mice were screened also for retinal degeneration due to Pde6brd1 homozygosity (Bowes et al., 1993), and only animals free of retinal degeneration were used. Ts65Dn and control (2N) mice were housed 2 to 5 per cage with a 12 hours light-dark cycle and *ad lib* access to food and water. Male littermate 3–4 month old mice were used in all studies. All the experiments were conducted in accordance with the National Institutes of Health guidelines for the care and use of animals and with an approved animal protocol from the Stanford University Institutional Animal Care and Use Committee.

### Slice preparation

Mice were anesthetized with isoflurane before decapitation. The brain was quickly removed and immersed for 2 min in ice-cold artificial cerebrospinal fluid (ACSF) containing 119 mM NaCl, 2.5 mM KCl, 1.3 mM $CaCl_2$, 2.5 mM $MgSO_4$, 1 mM $NaH_2PO_4$, 26 mM $NaHCO_3$, 10 mM glucose, osmolarity 310 mOsm, continuously bubbled with 95% $O_2$-5% $CO_2$, pH 7.4. The hippocampus was extracted and cut in ice-cold ACSF with a vibratome (Leica 1000) into 350-μm-thick transverse slices, which were allowed to recover in oxygenated ACSF at 35°C for 30 min, and then at room temperature for at least 1 h prior to experimental recordings. Slices prepared from the middle third of the hippocampus along the septo-temporal axis were used.

### Whole-cell recordings

Whole-cell currents of DG granule cells were recorded using an amplifier Axoclamp-2A (Axon Instruments, Union City, CA). The recordings were performed in ACSF containing (in mM): 119 NaCl, 2.5 KCl, 2 $CaCl_2$, 2 $MgSO_4$, 1 $NaH_2PO_4$, 26 $NaHCO_3$, 10 glucose and 5 μM of the AMPA receptor antagonist 2,3-dihydroxy-6-nitro-7-sulfamoylbenzo[f] quinoxaline-2,3-dione (NBQX,) and 50 μM of the NMDA receptor antagonist 2-amino-5-phosphonopentanoate (APV), osmolarity 310 mOsm, continuously bubbled with carbogen (95% $O_2$-5% $CO_2$), pH 7.4. In studies of whole-cell currents evoked by baclofen and synaptic double-component GABAA/GABAB receptor-dependent inhibitory postsynaptic potentials (IPSCs), the recording electrodes were filled with a solution containing (in mM): 125 K-gluconate, 10 KCl, 0.1 $CaCl_2$, 1 EGTA, 10 HEPES, 2 MgATP, 0.2 $Na_2$-GTP, osmolarity 295 mOsm, pH 7.3. Junction potential (−10 mV) was subtracted from the values of all measurements. Junction potentials were measured directly using the approach described in the application note “Liquid Junction Potential Corrections’ (Axon Instrument Ltd). Input resistance was measured by applying hyperpolarizing steps (40 ms, 10 mV) from a holding potential of −80 mV every 10 s throughout the experiment. Double-component GABAA/GABAB receptor-mediated IPSCs were evoked by a monopolar Pt/Ir electrode with a 100-μm-long exposed tip, wire diameter 25.4 μm (PTT0110, World Precision Instruments, Sarasota, FL). Because the size of synaptic responses depends strongly on the

relative positions of the stimulating and recording electrodes, special care was taken to place these electrodes in consistent locations of the dorsal (upper) DG blade: the recording electrode in the middle of the granule cell layer, and the stimulating electrode in the molecular layer, ~50 μm from the granule cell layer and ~80 μm from the recording electrode. Single or paired stimuli (interstimulus interval 20–150 ms) were applied every 30 s. In each given condition, 3–5 individual traces collected across the recording session were averaged and used for analysis. Temporal distribution of the traces was similar across animals and groups. Responses recorded at the beginning and at the end of the recording session were compared, and the experiment was rejected if the response amplitude changed more than 15%. Results of four experiments were rejected by these criteria. GABAA and GABAB receptor-mediated components of IPSCs were measured as the averaged amplitudes at latencies of 4–7 ms and 180–220 ms after the stimulus artifact respectively. This method of measurement was validated with two approaches. First, the components were isolated pharmacologically with applications of selective antagonists of the GABAA (picrotoxin, 100 μM) and/or GABAB (CGP55845, 2 μM) receptors. Second, GABAB receptor-mediated component was obtained with a subtraction of a single-exponent approximation of the descending earlier phase of IPSCs from a dual-component response (De Koninck and Mody, 1997). The shapes and amplitudes of the GABAB receptor-mediated components obtained with these two approaches were identical. The GABAB receptor-mediated components started with a ~10 ms delay, thus allowing for accurate evaluation of the GABAA receptor mediated component at the earlier latencies. The paired-pulse ratio (PPR) was calculated as the IPSC2/IPSC1, where IPSC1 is the amplitude of first evoked response and IPSC2 is the amplitude of the second synaptic response, measured after subtracting the ‘tail’ of the first response. Miniature IPSCs (mIPSCs) were recorded in ACSF containing 5 μM NBQX, 50 μM D-APV and 1 μM TTX. In these experiments, low-calcium ACSF (0.8 mM $Ca^{+2}$, 3.0 mM Mg) was used. The recording electrodes were filled with solution containing 135 mM CsCl, 2 mM $MgCl_2$, 2.5 mM EGTA, 10 mM HEPES, 2 mM MgATP, 0.2 mM $Na_2$-GTP and 2 mM QX-314, osmolarity 290 mOsm, pH 7.3, junction potential −16 mV. The frequency of mIPSCs was evaluated using the ‘MiniAnalysis’ program (Synaptosoft, Decatur, GA, USA). Spontaneous events were screened automatically with threshold amplitude of 7 pA. The amplitude of an event was calculated as the difference between the peak value (average of 1.0 ms of data around the event maximum) and the baseline (average of 2 ms of data preceding the first deflection from baseline). Each event was inspected visually before being accepted. The recordings were filtered at 1 kHz, digitized at 5 kHz, and stored in a computer.

### Immunohistochemistry

Mice were deeply anesthetized with sodium pentobarbital (200 mg/kg; i.p.; Abbott Laboratories) and transcardially perfused for 1 minute with 0.9% NaCl (10 ml), and then for 10 minutes with 4% paraformaldehyde in 0.1 M phosphate-buffered saline (PBS), pH 7.4. The brains were removed, kept in the same fixative for 2–3 days and then sectioned coronally at 100 μm with a Vibratome (series 1000, TPI, St. Louis, MO). Free-floating coronal sections were pre-incubated in 5% nonfat milk in PBS and then incubated overnight at 4°C with rabbit anti-glutamic acid decarboxylase 65 (GAD65; Chemicon, Temecula, CA; dilution 1:1000) as the primary antibody. The sections were then rinsed in PBS (20 minutes, three changes) and incubated for 1 hour at room temperature with biotinylated donkey anti-rabbit IgG (1:200; Jackson ImmunoResearch, West Grove, PA). After rinsing with PBS (20 minutes, three changes), sections were incubated with fluorescein isothiocyanate (FITC)-conjugated streptavidin (1:500; Jackson ImmunoResearch) for 1 hour at room temperature. Following further rinsing, the sections were mounted on microscope glass slides and coverslipped with 90% glycerol in phosphate buffer. Hippocampal sections from 2N and Ts65Dn mice were processed simultaneously, blinded to the genotype. In control

experiments, omitting primary antibodies eliminated immunoreactivity. Confocal microscopy was performed as described (Belichenko et al., 2004, 2009b). In brief, slices were examined and scanned in a Radiance 2000 confocal microscope (Bio-Rad, Hertfordshire, UK) attached to a Nikon Eclipse E800 fluorescence microscope. Stained sections were imaged within 10 μm of the surface, where maximum intensity of immunofluorescence was revealed. LaserSharp software (Bio-Rad) was used to establish optimal conditions for collecting images. The images were analyzed with ImageJ (NIH, USA). For each sublayer of DG, optical densities were measured in three randomly chosen locations (25×25 μm), and the results were averaged. The major criterion for selection of a region was absence of image distortions caused by eventual disruption of tissue during processing. Background fluorescence was estimated for each DG sublayer using 2N and Ts65Dn sections incubated without primary antibody and subtracted. All measurements and evaluations were performed by an experimenter blind to genotype. The results were then averaged across all slices for each genotype and presented for each DG sublayer as mean ± SEM.

### Western Blot

The hippocampi were dissected on an ice-cold preparation table and homogenized in RIPA buffer (50 mM Tris-HCl, 1% NP-40, 0.25% Na-deoxycholate, 150 mM NaCl, 1 mM EDTA, 1 mM PMSF, 1 mM $Na_3VO_4$, 1 mM NaF) with 1 mg/mL protease inhibitor cocktail (aprotinin, leupeptin, pepstatin). Two groups of mice with 2N/Ts65Dn sample numbers 12/10 and 5/5 were used for analysis. The protein concentrations were determined using BCA protein Assay kit (Pierce, Rockford, IL). β–Actin was used as a reference protein. 14 μL (1 mg/mL) of total protein per lane were loaded onto precast 4–12% Bis-Tris gels (Invitrogen, Carlsbad, CA), and separated by electrophoresis at 80 volts for ~3 hours. Proteins were transferred to polyvinylidene fluoride microporous membranes, and the membranes were blocked with 4% nonfat milk in TBS-T solution (20 mM Tris-HCl, 150 mM NaCl, 0.1% Tween-20, pH 7.6). Membranes were then incubated with one of rabbit polyclonal primary antibodies including: anti-GABAAα1 (1:200, Upstate Biothech.), anti-GABAAα2 (1:300, Sigma), anti-GABAAα3 (1:250, Sigma), anti-GABAAα5 (1:1000, Sigma), anti-GABAAγ2 (1:1000, Alpha Diagnostic), GABABR1a (1:1000, Alpha Diagnostic), anti-GABABR1b (1:1000, Chemicon Int), anti-Kir3.2 (1:200, Upstate) or anti-actin (1:1000, Upstate). The blots were washed in TBS-T (3 times × 10 min) followed by incubation with goat anti-rabbit IgG-HRP conjugates at a dilution of 1:10,000. The blots were washed in TBS-T and then developed with SuperSignal (Pierce, Rockford, IL). Immunoblots were scanned by a scanner Duoscan f40 (AGFA, NJ), and the images were analyzed with ImageJ (NIH, USA).

### Statistics

For all experiments, data are presented as mean ± SEM. In all comparisons, Students T-test was used and $p < 0.05$ was taken as statistically significant.

## Results

### Increased GABAA and GABAB receptor-mediated synaptic responses in Ts65Dn DG

Previous studies suggested that the efficiency of inhibitory neurotransmission could be enhanced in the hippocampus of DS model mice. Although a number of indirect evidence supported this suggestion, enhanced inhibitory neurotransmission was not yet demonstrated directly in electrophysiological experiments. To characterize signaling through synaptic GABAergic receptors in a DS model, we recorded dual-component GABAA/GABAB receptor-mediated IPSCs from DG granule cells of 2N and Ts65Dn mice (Fig. 1). The reversal potentials of the GABAA and GABAB receptor-mediated synaptic currents were

first evaluated (Fig. 1A). For the GABAA receptor-mediated currents the reversal potentials were in 2N: −78.6 ± 0.92 mV, n = 7, and in Ts65Dn: −76.8 ± 1.3 mV, n = 12 (p = 0.26). For the GABAB receptor-mediated currents the reversal potentials were in 2N: −92.6 ± 0.4 mV, n = 7; in Ts65Dn: −92.4 ± 1.0 mV, n = 12 (p = 0.46). Thus, the reversal potentials of the GABAA and GABAB receptor-mediated synaptic currents were not changed in Ts65Dn cells, and were similar to previously published measures (e.g., (Otis et al., 1993; Ling and Benardo, 1994; De Koninck and Mody, 1997).

We next compared the efficiency of the GABAergic synaptic signaling mediated by GABAA and GABAB receptors in 2N and Ts65Dn DG cells. Dual-component IPSCs were evoked by a sub-maximum current of 100 μA and were recorded at holding potentials of −70 mV or −120 mV. Averaged across all recorded neurons, the responses were considerably greater in Ts65Dn cells (Fig. 1B). At the holding potential of −70 mV, the magnitudes of the GABAA and GABAB receptor-mediated components were greater in Ts65Dn cells by 74% and 59%, and at the holding potential of −120 mV by 88% and 65% respectively. To examine the dependence of GABAA and GABAB receptor-mediated synaptic currents from the strength of afferent stimuli, we analyzed the input-output characteristics of dual-component IPSCs (Fig. 1C, D). The recordings were performed at a holding potential of -120 mV with stimulating currents ranging from 30 to 300 μA. As can be seen from representative recordings (Fig. 1C) and averaged data (Fig. 1D), the responses were significantly greater in Ts65Dn cells at all stimulus strengths. Averaged across all stimulus strengths, the GABAA and GABAB receptor-mediated responses were increased in Ts65Dn cells approximately by 132% and 123% respectively.

## Similarity in the distribution of GABAergic afferents and in the levels of GABAergic receptors in the DG of Ts65Dn mice

A number of mechanisms could potentially account for the increased inhibitory efficiency in Ts65Dn DG. One potential possibility is a change in the number or distribution of GABAergic synapses and/or receptors in Ts65Dn mice. Thus, it was observed recently that the level of GAD67, a marker of GABAergic neurons, was increased in the neocortex of Ts65Dn (Perez-Cremades et al., 2010). To evaluate distribution of GABAergic fibers in the Ts65Dn DG, we used immunostaining for GAD65, a variant of glutamic acid decarboxylase prominently expressed in the axonal terminals of GABAergic neurons. The intensity of immunofluorescence was examined throughout the DG layers. While there was variation across the layers, we found no difference when comparing data from 2N and Ts65Dn slices (Fig. 2). Thus, the outer molecular layer immunostaining for GAD65 had a tendency to be even lower in Ts65Dn (Fig. 2A, insert), but the difference did not reach the significance level (p = 0.19) (Fig. 2B).

Next, hippocampal levels of the proteins involved in signaling through GABAergic receptors were evaluated using Western blot. There was no significant change in the levels of GABAA (α1, α2, α3, α5 and γ2) and GABAB (GBR1a and GBR1b) receptor subunits in the Ts65Dn vs. 2N hippocampal samples, although the level of α1 subunit showed a trend for reduction (p = 0.09) (Table 1 for averaged data; Supplementary Fig. S1 and S2 for examples of immunoblots). Levels of GAT-1, a GABA transporter prominently expressed in the hippocampus, and actin were also unchanged. In contrast, the level of the Kir3.2 subunit of potassium channels that serve as effectors for postsynaptic GABAB receptors was significantly increased in Ts65Dn samples (2N: 100 ± 9.0%, n = 9; Ts65Dn: 159.0 ± 12.2%, n = 9; p = 0.0008) (Table 1). Thus, we found no evidence for changes in the distribution of GABAergic synapses or in the levels of GABAA or GABAB receptor subunits that would explain the increase in GABAergic signaling in the Ts65Dn DG. However, we observed an increase in Kir3.2 subunits that could contribute to an enhanced signaling through postsynaptic GABAB receptors.

### Changes of presynaptic GABAergic terminals in Ts65Dn DG

It is possible that enhanced inhibitory efficiency in the Ts65Dn DG may reside, at least in part, in alterations of individual GABAergic synapses. To test the properties of GABAergic terminals, we first examined paired-pulse plasticity of dual-component IPSCs (Fig. 3). At interstimulus intervals of 20 ms and 50 ms, PPR values of both GABAA and GABAB receptor-mediated components were smaller in the Ts65Dn DG (Fig. 3A). Thus, at an interstimulus interval of 20 ms, the PPR values were for the GABAA receptor-mediated IPSCs 0.85 ± 0.06 and 0.60 ± 0.04 ($p = 0.003$), and for the GABAB receptor-mediated IPSCS 0.88 ± 0.07 and 0.64 ± 0.07 ($p = 0.03$, $n = 4–7$) in 2N and Ts65Dn cells respectively (Fig. 3B). Although paired-pulse plasticity has mainly a presynaptic origin, some postsynaptic factors may affect PPR values. Thus, GABAB receptor-mediated K+ conductance triggered by the first stimulus could shunt the second IPSC and, hence, reduce the PPR values. Because GABAB receptor-mediated responses are bigger in Ts65Dn cells, the reduction in PPR could be greater. To examine whether or not postsynaptic GABAB receptor-mediated conductivity explains smaller PPR values in Ts65Dn cells, we examined paired-pulse plasticity in the presence of GABAB receptor-antagonist CGP55845 (4 μM) with use of Cs+-filled recording electrodes. To reduce activation of other fibers that could potentially affect postsynaptic currents and, hence, PPR values, low calcium ACSF and weak afferent stimuli (20–30 μA) were used. At these conditions, PPR was still lower in Ts65Dn cells (2N: 1.60 ± 0.11 %, $n = 5$; Ts65Dn: 1.29 ± 0.07 %, $n = 5$, $p = 0.023$). Thus, changes of presynaptic GABAergic terminals are likely responsible for reduced PPR of IPSCs in Ts65Dn DG.

Release of GABA could be affected by a number of presynaptic receptors, including the GABAB receptors (Davies and Collingridge, 1993). To examine properties of presynaptic GABAB receptors in Ts65Dn DG, we first measured effects of the GABAB receptor agonist baclofen (40 μM) on the frequency of miniature IPSCs (mIPSCs) (Fig. 4). Representative recordings (Fig. 4A) and averaged data (Fig. 4B) showed that the baseline frequency of mIPSCs was significantly greater in Ts65Dn granule cells (2N: 2.38 ± 0.34 Hz, $n = 5$; Ts65Dn: 3.42 ± 0.39 Hz, $n = 5$; $p = 0.027$). Application of baclofen reduced the frequency of mIPSCs, but the effects were similar in 2N and Ts65Dn cells (2N: 40.2 ± 5.2%, $n = 5$; Ts65Dn: 41.0 ± 3.1%, $n = 5$, $p = 0.44$) (Fig. 4C). Another parameter strongly affected by presynaptic GABAB receptors is PPR of IPSCs at an interstimulus interval of ~150 ms. We observed that this parameter was not altered in Ts65Dn DG for both the GABAA and GABAB receptor-mediated IPSC components ($p < 0.4$) (Fig. 3). Thus, the results suggest that the efficiency of presynaptic GABAB receptors is not changed in Ts65Dn DG.

### Hyperpolarized resting membrane potential and enhanced postsynaptic GABAB/Kir3.2 signaling in Ts65Dn vs. 2N granule cells

An increase in the expression level of the Kir3.2 subunits of potassium channels in Ts65Dn mice could affect a number of neuronal properties, including resting membrane potential. Because the equilibrium potential for potassium ions is more negative than the resting membrane potential, increased potassium currents would result in hyperpolarization of neurons. To test for this change, we compared resting membrane potentials in 2N and Ts65Dn DG granule cells. We observed that membrane potential was more negative in Ts65Dn cells (2N: −72.7 ± 2.2 mV, $n = 19$; Ts65Dn: −78.4 ± 2.2 mV, $n = 11$; $p = 0.045$), while the values for input resistance were not altered (2N: 411.9 ± 40.4 MΩ, $n = 9$; Ts65Dn: 340.4 ± 25.7 MΩ, $n = 7$; $p = 0.44$).

Another consequence of an increase in the Kir3.2 protein could be enhanced signaling through postsynaptic GABAB receptors, since these metabotropic receptors use Kir3.2 subunit-containing potassium channels as effectors. Such an enhancement was observed

previously in primary cultured neurons from Ts65Dn hippocampus (Best et al., 2007). To examine signaling through the GABAB receptors in adult mice, we measured whole-cell currents and changes in input resistance of granule cells during bath application of the selective GABAB receptor agonist baclofen (40 μM). Application of baclofen resulted in the generation of outward currents (Fig. 5A) and in reduction of input resistance (Fig. 5B). Both these effects were greater in Ts65Dn cells. On average, whole-cell currents evoked by baclofen were in 2N: 10.2 ± 2.7 pA, n = 7; in Ts65Dn: 17.9 ± 3.7 pA, n = 7 ($p = 0.047$). Changes of input resistance were in 2N: 41.01 ± 3.62%, n = 7; in Ts65Dn: 51.31 ± 2.72%, n = 7 ($p = 0.029$). Thus, the increased expression level of Kir3.2 protein is associated with excessive hyperpolarization and enhanced signaling through the postsynaptic GABAB receptors in Ts65Dn DG granule cells.

## Discussion

DS results in several phenotypes reflecting cognitive dysfunction and intellectual disability. In the Ts65Dn model of DS, imbalance of excitation and inhibition contributes to abnormal synaptic plasticity and memory. Here we present first direct electrophysiological evidence of enhanced synaptic GABAergic efficiency in Ts65Dn DG. This enhancement was associated with reduced paired-pulse ratio of evoked IPSCs, suggesting an increased presynaptic release of GABA, and with increased postsynaptic GABAB/Kir3.2 signaling. No evident morphological or biochemical changes of the GABAergic system have been observed. The results suggest that changes at the level of individual GABAergic synapses could be responsible for the enhanced inhibitory efficiency in Ts65Dn mice.

Previous studies in DS model mice suggested imbalance of excitation and inhibition in favor of the latter (Kleschevnikov et al., 2004; Costa and Grybko, 2005; Fernandez et al., 2007; Belichenko et al., 2009b). Hypothetically, such an imbalance could arise from changes in excitatory, inhibitory, or both of these systems. Because no change was observed in the efficiency of glutamatergic neurotransmission (Siarey et al., 1997; Kleschevnikov et al., 2004; Costa and Grybko, 2005; Fernandez and Garner, 2007), increased GABAergic efficiency appeared as the most likely scenario. Multiple observations revealed changes in the GABAergic system (Kleschevnikov et al., 2004; Fernandez et al., 2007; Belichenko et al., 2009b; Perez-Cremades et al., 2010). Thus, alteration in the microcircuitry of inhibitory inputs with a significant increase in inputs to the necks of spines was observed in the DG of DS model mice (Belichenko et al., 2007). Density of parvalbumin- and somatostatin-positive GABAergic neurons was reportedly increased in the hippocampus of juvenile Ts65Dn mice, possibly due to increased expression of *Olig1* and *Olig2* genes (Chakrabarti et al., 2010). Interestingly, neither electron microscopy nor immunostaining studies found changes in the density of inhibitory synapses in adult Ts65Dn DG (Belichenko et al., 2009b). Consistent with these data, herein we observed that immunostaining for GAD65, a form of GAD prominently expressed in GABAergic terminals (Kaufman et al., 1991; Martin and Rimvall, 1993), was not altered in Ts65Dn DG. Likewise, no difference was observed in levels of major subunits of GABAergic receptors or in GAT-1, a GABA transporter prominently expressed in the hippocampus. These findings are consistent with our previous observations (Belichenko et al., 2009b) and suggest that the number and distribution of GABAergic synapses and receptors are not substantially altered in the DG of adult Ts65Dn mice.

Another explanation for the over-inhibition could be a change of individual GABAergic synapses. One suggested mechanism for such changes is enhanced presynaptic release of GABA Consistent with this suggestion paired-pulse ratio of evoked IPSCs was significantly smaller in Ts65Dn DG for both GABAA and GABAB IPSC components. This result is consistent with reduced paired-pulse facilitation of IPCSs observed at reduced

neurotransmitter release conditions (Kleschevnikov et al., 2004). Although paired-pulse plasticity of evoked responses depends from many factors, including those with postsynaptic origin (e.g., (Wang and Kelly, 1997), this effect has mainly a presynaptic origin depending on presynaptic release probability (Zucker, 1989). Since neurotransmitter release probability is inversely related to PPR values, these results suggest that release probability of GABA is increased in Ts65Dn DG. Increased frequency of mIPSCs in Ts65Dn cells provides additional support to this idea. Indeed, because the density of inhibitory synapses is not significantly altered in Ts65Dn DG (Belichenko et al., 2009b), a likely explanation for changes in mIPSCs frequency is an enhancement in GABA release probability. One factor affecting the release probability is size of synapses. Indeed, larger synapses generally show greater values of release probability (Murthy et al., 2001), possibly due to increased vesicle availability. Consistent with such a possibility, we observed in a recent electron microscopy study that the size of symmetric (presumably inhibitory) synapses is increased in Ts65Dn DG (Belichenko et al., 2009b).

Level of the Kir3.2 (Girk2) subunits of inwardly-rectifying potassium channels was increased by ~50% in the hippocampus of Ts65Dn mice, a finding consistent with earlier observations (Kleschevnikov et al., 2005; Harashima et al., 2006). Kir3.2 protein is encoded by *KCNJ6*, a gene located in the so-called ‘Down syndrome critical region’. A number of metabotropic receptors use Kir3.2 subunit-containing potassium channels as postsynaptic effectors (Luscher et al., 1997). Expression levels of the Kir3.2 protein may affect signaling through these receptors and other neuronal properties, including resting membrane potential (Dascal, 1997; Luscher et al., 1997; Mark and Herlitze, 2000). Consistent with the increase in Kir3.2 protein, we observed more negative resting membrane potential in the Ts65Dn DG granule cells. GABAB agonist baclofen produced significantly greater whole-cell currents and a larger reduction in input resistance of Ts65Dn DG granule cells. Of note, in spite of the change in the resting membrane potential and baclofen-evoked currents, we observed no significant changes in input resistance in Ts65Dn vs. 2N cells. Because with a current pulse one measures mainly soma resistance, these results suggest that the additional Kir3.2 channels in Ts65Dn may be located mostly in dendrites. Consistent with this suggestion, CA1 pyramidal neurons of Kir3.2 knock-out mice also exhibited changes in membrane potential, but no change in input resistance, compared to WT controls (Koyrakh et al., 2005). Thus, consistent with earlier observations in primary cultured hippocampal neurons (Best et al., 2007; Cramer et al., 2010), postsynaptic GABAB/Kir3.2 signaling is enhanced in DG of adult Ts65Dn mice.

In experiments with dual component IPSCs, we observed that both GABAA and GABAB receptor-mediated components were significantly increased in Ts65Dn DG. Are those changes consistent with the enhancement of GABAB/Kir3.2 signaling, which should selectively affect the GABAB component? A possible explanation of this discrepancy could be as following. As discussed above, an increase in presynaptic release of GABA could be a result of an increased size of GABAergic synapses in Ts65Dn DG. GABAA and GABAB receptors are differently distributed across the synaptic area and, therefore, the corresponding IPSC components should be differently affected by increases of synaptic area. GABAA receptors occupy the entire postsynaptic area, with a sharp decrease at the edge of synaptic membrane specialization (Nusser et al., 1995; Somogyi et al., 1996). Assuming a circular synaptic area with radius $R$, GABAA receptor-mediated component of IPSC should be increased proportionally to the area, i.e. as $\sim R^2$. In contrast, GABAB receptors are mostly located at the periphery of the synaptic area (Kulik et al., 2003; Ulrich and Bettler, 2007), and the corresponding currents should rise proportionally to the length of the circumference, i.e. as $\sim R$. We observed a 2.32 fold increase of the GABAA receptor-mediated IPSC component. Assuming that this change is caused by an increase in synaptic area, the corresponding increase for the GABAB component would be 1.52 fold (i.e. $\sqrt{2}.32$).

The observed increase of the GABAB receptor mediated component of IPSCS in Ts65Dn DG was actually 2.23 fold, a value 48% greater than predicted (2.23/1.52 = 1.48). The additional increase in the efficiency of postsynaptic GABAB/Kir3.2 signaling is consistent with the increased availability of the Kir3.2 subunit-containing potassium channels.

Changes in inhibitory efficiency could result from DS-specific genetic abnormalities or from compensatory alterations during development. In addition to genes discussed above, a number of other triplicated genes could potentially affect the morphology and function of GABAergic terminals. Synaptojanin 1 (*Synj1*), a nerve terminal protein implicated in the endocytosis (Mcpherson et al., 1994), influences the stability of GABAergic transmission (Luthi et al., 2001). Intersectin 1 (*Itsn1*), an adaptor protein overexpressed in DS (Pucharcos et al., 1999), is also involved in endocytosis (Schafer, 2002). Up-regulation of GABAergic neurotransmission was observed in mice overexpressing superoxide dismutase 1 (*Sod1*) (Levkovitz et al., 1999). *Dyrk1A, Tiam1, Dscr1* and *Dscam* have all been implicated in altered synaptic function (Agarwala et al., 2000; Tolias et al., 2007; Chang and Min, 2009; Murakami et al., 2009) and could contribute to changes in inhibitory efficiency described in this study.

In conclusion, in exploring the mechanisms of increased inhibition in the DG of Ts65Dn mice we found that both GABAA and GABAB receptor-mediated signaling was impacted significantly. These results suggest that antagonists of the GABAA and GABAB receptors, as well as blockers of Kir3.2-containing potassium channels should be explored as potential medicines for improving learning and memory in people with DS.

### Highlights

Synaptic GABAergic efficiency was examined in Ts65Dn mouse model of Down syndrome - Both GABAA and GABAB IPSC components were significantly increased - Hippocampal levels of subunits of GABAergic receptors were unchanged - Paired-pulse ratio of IPSCs was reduced suggesting increased release of GABA - Postsynaptic GABAB/Kir3.2 signaling was increased in Ts65Dn dentate gyrus-Changes in inhibitory efficiency are likely responsible for reduced cognition in DS

## Supplementary Material

Refer to Web version on PubMed Central for supplementary material.

## REFERENCES

Agarwala KL, Nakamura S, Tsutsumi Y, Yamakawa K. Down syndrome cell adhesion molecule DSCAM mediates homophilic intercellular adhesion. Brain Res Mol Brain Res. 2000; 79:118–126. [PubMed: 10925149]

Belichenko NP, Belichenko PV, Kleschevnikov AM, Salehi A, Reeves RH, Mobley WC. The "Down syndrome critical region" is sufficient in the mouse model to confer behavioral, neurophysiological, and synaptic phenotypes characteristic of Down syndrome. J Neurosci. 2009a; 29:5938–5948. [PubMed: 19420260]

Belichenko PV, Kleschevnikov AM, Masliah E, Wu C, Takimoto-Kimura R, Salehi A, Mobley WC. Excitatory-inhibitory relationship in the fascia dentata in the Ts65Dn mouse model of Down syndrome. J Comp Neurol. 2009b; 512:453–466. [PubMed: 19034952]

Belichenko PV, Kleschevnikov AM, Salehi A, Epstein CJ, Mobley WC. Synaptic and cognitive abnormalities in mouse models of Down syndrome: exploring genotype-phenotype relationships. J Comp Neurol. 2007; 504:329–345. [PubMed: 17663443]

Belichenko PV, Masliah E, Kleschevnikov AM, Villar AJ, Epstein CJ, Salehi A, Mobley WC. Synaptic structural abnormalities in the Ts65Dn mouse model of Down Syndrome. J Comp Neurol. 2004; 480:281–298. [PubMed: 15515178]

Best TK, Siarey RJ, Galdzicki Z. Ts65Dn, a mouse model of Down syndrome, exhibits increased GABAB-induced potassium current. J Neurophysiol. 2007; 97:892–900. [PubMed: 17093127]

Bowes C, Li T, Frankel WN, Danciger M, Coffin JM, Applebury ML, Farber DB. Localization of a retroviral element within the rd gene coding for the beta subunit of cGMP phosphodiesterase. Proc Natl Acad Sci U S A. 1993; 90:2955–2959. [PubMed: 8385352]

Carlesimo GA, Marotta L, Vicari S. Long-term memory in mental retardation: evidence for a specific impairment in subjects with Down's syndrome. Neuropsychologia. 1997; 35:71–79. [PubMed: 8981379]

Chakrabarti L, Best TK, Cramer NP, Carney RS, Isaac JT, Galdzicki Z, Haydar TF. Olig1 and Olig2 triplication causes developmental brain defects in Down syndrome. Nat Neurosci. 2010

Chang KT, Min KT. Upregulation of three Drosophila homologs of human chromosome 21 genes alters synaptic function: implications for Down syndrome. Proc Natl Acad Sci U S A. 2009; 106:17117–17122. [PubMed: 19805187]

Costa AC, Grybko MJ. Deficits in hippocampal CA1 LTP induced by TBS but not HFS in the Ts65Dn mouse: a model of Down syndrome. Neurosci Lett. 2005; 382:317–322. [PubMed: 15925111]

Coyle JT, Oster-Granite ML, Reeves R, Hohmann C, Corsi P, Gearhart J. Down syndrome and the trisomy 16 mouse: impact of gene imbalance on brain development and aging. Res Publ Assoc Res Nerv Ment Dis. 1991; 69:85–99. [PubMed: 1825889]

Cramer NP, Best TK, Stoffel M, Siarey RJ, Galdzicki Z. GABAB-GIRK2-mediated signaling in Down syndrome. Adv Pharmacol. 2010; 58:397–426. [PubMed: 20655490]

Dascal N. Signalling via the G protein-activated K+ channels. Cell Signal. 1997; 9:551–573. [PubMed: 9429760]

Davies CH, Collingridge GL. The physiological regulation of synaptic inhibition by GABAB autoreceptors in rat hippocampus. J Physiol. 1993; 472:245–265. [PubMed: 8145143]

Davies CH, Starkey SJ, Pozza MF, Collingridge GL. GABA autoreceptors regulate the induction of LTP. Nature. 1991; 349:609–611. [PubMed: 1847993]

Davisson MT, Schmidt C, Reeves RH, Irving NG, Akeson EC, Harris BS, Bronson RT. Segmental trisomy as a mouse model for Down syndrome. Prog Clin Biol Res. 1993; 384:117–133. [PubMed: 8115398]

De Koninck Y, Mody I. Endogenous GABA activates small-conductance K+ channels underlying slow IPSCs in rat hippocampal neurons. J Neurophysiol. 1997; 77:2202–2208. [PubMed: 9114267]

Dierssen M, Fillat C, Crnic L, Arbones M, Florez J, Estivill X. Murine models for Down syndrome. Physiol Behav. 2001; 73:859–871. [PubMed: 11566219]

Dorostkar MM, Boehm S. Presynaptic lonotropic receptors. Handb Exp Pharmacol. 2008:479–527. [PubMed: 18064423]

Fernandez F, Garner CC. Over-inhibition: a model for developmental intellectual disability. Trends Neurosci. 2007; 30:497–503. [PubMed: 17825437]

Fernandez F, Morishita W, Zuniga E, Nguyen J, Blank M, Malenka RC, Garner CC. Pharmacotherapy for cognitive impairment in a mouse model of Down syndrome. Nat Neurosci. 2007; 10:411–413. [PubMed: 17322876]

Fink KB, Gothert M. 5-HT receptor regulation of neurotransmitter release. Pharmacol Rev. 2007; 59:360–417. [PubMed: 18160701]

Galdzicki Z, Siarey RJ. Understanding mental retardation in Down's syndrome using trisomy 16 mouse models. Genes Brain Behav. 2003; 2:167–178. [PubMed: 12931790]

Gardiner K, Fortna A, Bechtel L, Davisson MT. Mouse models of Down syndrome: how useful can they be? Comparison of the gene content of human chromosome 21 with orthologous mouse genomic regions. Gene. 2003; 318:137–147. [PubMed: 14585506]

Hanson JE, Blank M, Valenzuela RA, Garner CC, Madison DV. The functional nature of synaptic circuitry is altered in area CA3 of the hippocampus in a mouse model of Down's syndrome. J Physiol. 2007; 579:53–67. [PubMed: 17158177]

Harashima C, Jacobowitz DM, Witta J, Borke RC, Best TK, Siarey RJ, Galdzicki Z. Abnormal expression of the G-protein-activated inwardly rectifying potassium channel 2 (GIRK2) in hippocampus, frontal cortex, and substantia nigra of Ts65Dn mouse: a model of Down syndrome. J Comp Neurol. 2006; 494:815–833. [PubMed: 16374808]

Holtzman DM, Santucci D, Kilbridge J, Chua-Couzens J, Fontana DJ, Daniels SE, Johnson RM, Chen K, Sun Y, Carlson E, Alleva E, Epstein CJ, Mobley WC. Developmental abnormalities and age-related neurodegeneration in a mouse model of Down syndrome. Proc Natl Acad Sci U S A. 1996; 93:13333–13338. [PubMed: 8917591]

Kaufman DL, Houser CR, Tobin AJ. Two forms of the gamma-aminobutyric acid synthetic enzyme glutamate decarboxylase have distinct intraneuronal distributions and cofactor interactions. J Neurochem. 1991; 56:720–723. [PubMed: 1988566]

Kleschevnikov AM, Belichenko PV, Villar AJ, Epstein CJ, Malenka RC, Mobley WC. Hippocampal long-term potentiation suppressed by increased inhibition in the Ts65Dn mouse, a genetic model of Down syndrome. J Neurosci. 2004; 24:8153–8160. [PubMed: 15371516]

Kleschevnikov, AM.; Van Volkinburg, J.; Zhan, K.; Mobley, WC. Abstract Viewer/Itinerary Planner. Washington, DC: Society for Neuroscience; 2005. Expression of GIRK2 and related proteins after chronic administrations of Prozac in Ts65Dn mice, a genetic model of Down syndrome. Program No. 115.7.

Koyrakh L, Lujan R, Colon J, Karschin C, Kurachi Y, Karschin A, Wickman K. Molecular and cellular diversity of neuronal G-protein-gated potassium channels. J Neurosci. 2005; 25:11468–11478. [PubMed: 16339040]

Kulik A, Vida I, Lujan R, Haas CA, Lopez-Bendito G, Shigemoto R, Frotscher M. Subcellular localization of metabotropic GABA(B) receptor subunits GABA(B1a/b) and GABA(B2) in the rat hippocampus. J Neurosci. 2003; 23:11026–11035. [PubMed: 14657159]

Levkovitz Y, Avignone E, Groner Y, Segal M. Upregulation of GABA neurotransmission suppresses hippocampal excitability and prevents long-term potentiation in transgenic superoxide dismutase-overexpressing mice. J Neurosci. 1999; 19:10977–10984. [PubMed: 10594078]

Ling DS, Benardo LS. Properties of isolated GABAB-mediated inhibitory postsynaptic currents in hippocampal pyramidal cells. Neuroscience. 1994; 63:937–944. [PubMed: 7535398]

Luscher C, Jan LY, Stoffel M, Malenka RC, Nicoll RA. G protein-coupled inwardly rectifying K+ channels (GIRKs) mediate postsynaptic but not presynaptic transmitter actions in hippocampal neurons. Neuron. 1997; 19:687–695. [PubMed: 9331358]

Luthi A, Di Paolo G, Cremona O, Daniell L, De Camilli P, McCormick DA. Synaptojanin 1 contributes to maintaining the stability of GABAergic transmission in primary cultures of cortical neurons. J Neurosci. 2001; 21:9101–9111. [PubMed: 11717343]

Mark MD, Herlitze S. G-protein mediated gating of inward-rectifier K+ channels. Eur J Biochem. 2000; 267:5830–5836. [PubMed: 10998041]

Martin DL, Rimvall K. Regulation of gamma-aminobutyric acid synthesis in the brain. J Neurochem. 1993; 60:395–407. [PubMed: 8419527]

McPherson PS, Takei K, Schmid SL, De Camilli P. p145, a major Grb2-binding protein in brain, is co-localized with dynamin in nerve terminals where it undergoes activity-dependent dephosphorylation. J Biol Chem. 1994; 269:30132–30139. [PubMed: 7982917]

Moore CS, Roper RJ. The power of comparative and developmental studies for mouse models of Down syndrome. Mamm Genome. 2007; 18:431–443. [PubMed: 17653795]

Murakami N, Bolton D, Hwang YW. Dyrk1A binds to multiple endocytic proteins required for formation of clathrin-coated vesicles. Biochemistry. 2009; 48:9297–9305. [PubMed: 19722700]

Murthy VN, Schikorski T, Stevens CF, Zhu Y. Inactivity produces increases in neurotransmitter release and synapse size. Neuron. 2001; 32:673–682. [PubMed: 11719207]

Nusser Z, Roberts JD, Baude A, Richards JG, Sieghart W, Somogyi P. Immunocytochemical localization of the alpha 1 and beta 2/3 subunits of the GABAA receptor in relation to specific GABAergic synapses in the dentate gyrus. Eur J Neurosci. 1995; 7:630–646. [PubMed: 7620614]

Olson LE, Roper RJ, Sengstaken CL, Peterson EA, Aquino V, Galdzicki Z, Siarey R, Pletnikov M, Moran TH, Reeves RH. Trisomy for the Down syndrome 'critical region' is necessary but not

sufficient for brain phenotypes of trisomic mice. Hum Mol Genet. 2007; 16:774–782. [PubMed: 17339268]

Otis TS, De Koninck Y, Mody I. Characterization of synaptically elicited GABAB responses using patch-clamp recordings in rat hippocampal slices. J Physiol. 1993; 463:391–407. [PubMed: 8246190]

Perez-Cremades D, Hernandez S, Blasco-Ibanez JM, Crespo C, Nacher J, Varea E. Alteration of inhibitory circuits in the somatosensory cortex of Ts65Dn mice, a model for Down's syndrome. J Neural Transm. 2010; 117:445–455. [PubMed: 20157742]

Pucharcos C, Fuentes JJ, Casas C, de la Luna S, Alcantara S, Arbones ML, Soriano E, Estivill X, Pritchard M. Alu-splice cloning of human Intersectin (ITSN), a putative multivalent binding protein expressed in proliferating and differentiating neurons and overexpressed in Down syndrome. Eur J Hum Genet. 1999; 7:704–712. [PubMed: 10482960]

Reeves RH. Down syndrome mouse models are looking up. Trends Mol Med. 2006; 12:237–240. [PubMed: 16677859]

Roizen NJ, Patterson D. Down's syndrome. Lancet. 2003; 361:1281–1289. [PubMed: 12699967]

Rueda N, Florez J, Martinez-Cue C. Chronic pentylenetetrazole but not donepezil treatment rescues spatial cognition in Ts65Dn mice, a model for Down syndrome. Neurosci Lett. 2008; 433:22–27. [PubMed: 18226451]

Salehi A, Delcroix JD, Belichenko PV, Zhan K, Wu C, Valletta JS, Takimoto-Kimura R, Kleschevnikov AM, Sambamurti K, Chung PP, Xia W, Villar A, Campbell WA, Kulnane LS, Nixon RA, Lamb BT, Epstein CJ, Stokin GB, Goldstein LS, Mobley WC. Increased App expression in a mouse model of Down's syndrome disrupts NGF transport and causes cholinergic neuron degeneration. Neuron. 2006; 51:29–42. [PubMed: 16815330]

Salehi A, Faizi M, Belichenko PV, Mobley WC. Using mouse models to explore genotype-phenotype relationship in Down syndrome. Ment Retard Dev Disabil Res Rev. 2007; 13:207–214. [PubMed: 17910089]

Salehi A, Faizi M, Colas D, Valletta JS, Laguna J, Takimoto-Kimura R, Kleschevnikov AM, Wagner SL, Aizen P, Shamloo M, Mobley WC. Restoration of norepinephrine-modulated contextual memory in a mouse model of Down syndrome. Science Transl Med. 2009; 1:7–17.

Schafer DA. Coupling actin dynamics and membrane dynamics during endocytosis. Curr Opin Cell Biol. 2002; 14:76–81. [PubMed: 11792548]

Siarey RJ, Stoll J, Rapoport SI, Galdzicki Z. Altered long-term potentiation in the young and old Ts65Dn mouse, a model for Down Syndrome. Neuropharmacology. 1997; 36:1549–1554. [PubMed: 9517425]

Somogyi P, Fritschy JM, Benke D, Roberts JD, Sieghart W. The gamma 2 subunit of the GABAA receptor is concentrated in synaptic junctions containing the alpha 1 and beta 2/3 subunits in hippocampus, cerebellum and globus pallidus. Neuropharmacology. 1996; 35:1425–1444. [PubMed: 9014159]

Sturgeon X, Gardiner KJ. Transcript catalogs of human chromosome 21 and orthologous chimpanzee and mouse regions. Mamm Genome. 2011; 22:261–271. [PubMed: 21400203]

Tolias KF, Bikoff JB, Kane CG, Tolias CS, Hu L, Greenberg ME. The Rac1 guanine nucleotide exchange factor Tiam1 mediates EphB receptor-dependent dendritic spine development. Proc Natl Acad Sci U S A. 2007; 104:7265–7270. [PubMed: 17440041]

Ulrich D, Bettler B. GABA(B) receptors: synaptic functions and mechanisms of diversity. Curr Opin Neurobiol. 2007; 17:298–303. [PubMed: 17433877]

Wang JH, Kelly PT. Attenuation of paired-pulse facilitation associated with synaptic potentiation mediated by postsynaptic mechanisms. J Neurophysiol. 1997; 78:2707–2716. [PubMed: 9356420]

Zucker RS. Short-term synaptic plasticity. Annu Rev Neurosci. 1989; 12:13–31. [PubMed: 2648947]

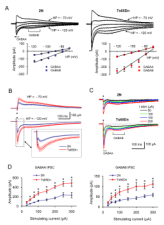

**Figure 1.**

Double-component GABAA/GABAB receptor-mediated IPSCs in 2N and Ts65Dn DG. (A) Reversal potentials for the GABAA and GABAB receptor-mediated components of IPSCs. Examples on top are the whole-cell currents recorded at holding potentials (HP) ranging from −70 mV to −120 mV. Graphs show the current-voltage relationship for the GABAA and GABAB receptor-mediated components of IPSCs in 2N (left) and Ts65Dn (right) cells. The reversal potentials of both components were similar in 2N and Ts65Dn cells. (B) Averaged double-component IPSCs recorded at holding potentials of −70 mV (top) and −120 mV (bottom) in 2N (n = 9) and Ts65Dn (n = 12) cells. The thin lines show mean ± SEM. Insert: the expanded view of the responses showing the details of the GABAA receptor-mediated component. (C) Examples of whole cell currents evoked in 2N and Ts65Dn cells. The recordings were performed at holding potential of −120 mV. (D) Magnitudes of the GABAA (left) and GABAB (right) receptor-mediated IPSC components as function of the stimulating current. The recordings were performed at holding potential of −120 mV. Both GABAA and GABAB receptor-mediated IPSC components were significantly greater in Ts65Dn cells. * $p < 0.01$.

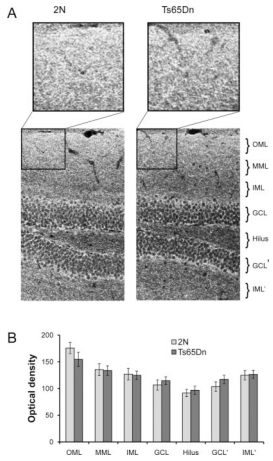


**Figure 2.**

Immunostaining for GAD65 in 2N and Ts65Dn DG. (A) Examples of immunofluorescence in 2N (left) and Ts65Dn (right) DG. Insert on top: Examples of immunofluorescence in IML at higher magnification. Note a tendency for a lower level of GAD65 in Ts65Dn. (B) Averaged values for the immunofluorescence intensity (arbitrary units) across the DG layers. Immunofluorescence was maximal in the outer molecular layer (OML), gradually reduced in the middle and inner molecular layers (MML and IML) and reached a minimum in the granule cell layer (GCL) and hilus. GCL' and IML' are the layers from the inferior (lower) blade of the DG. There was no significant difference between 2N and Ts65Dn DG layers ($p > 0.2$).

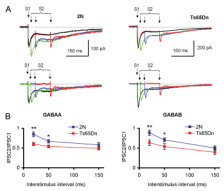

**Figure 3.**

Paired-pulse plasticity of GABAA and GABAB receptor-mediated components of IPSC. (A) Top panel: Examples of double-component GABAA/GABAB receptor-mediated IPSCs evoked by paired stimuli (S1 and S2) with interstimuli intervals 20 ms, 50 ms and 150 ms in 2N (left) and Ts65Dn (right) cells. The responses evoked by a single stimulus are shown in black, while the responses evoked by paired stimuli are colored. Bottom panel: responses to the second stimulus in the pair obtained by subtracting of the single-stimulus response (black) from the corresponding paired responses. Note smaller magnitude of the second stimulus responses relative to the first response in Ts65Dn cells. (B) Quantification of the data. PPR values of both GABAA (left) and GABAB (right) receptor-mediated IPSC components were significantly smaller in Ts65Dn cells for the short (20 ms and 50 ms) interstimulus intervals. No difference in PPR values was observed for the longer (150 ms) interval. *$p < 0.05$; **$p < 0.03$ (2N vs. Ts65Dn).

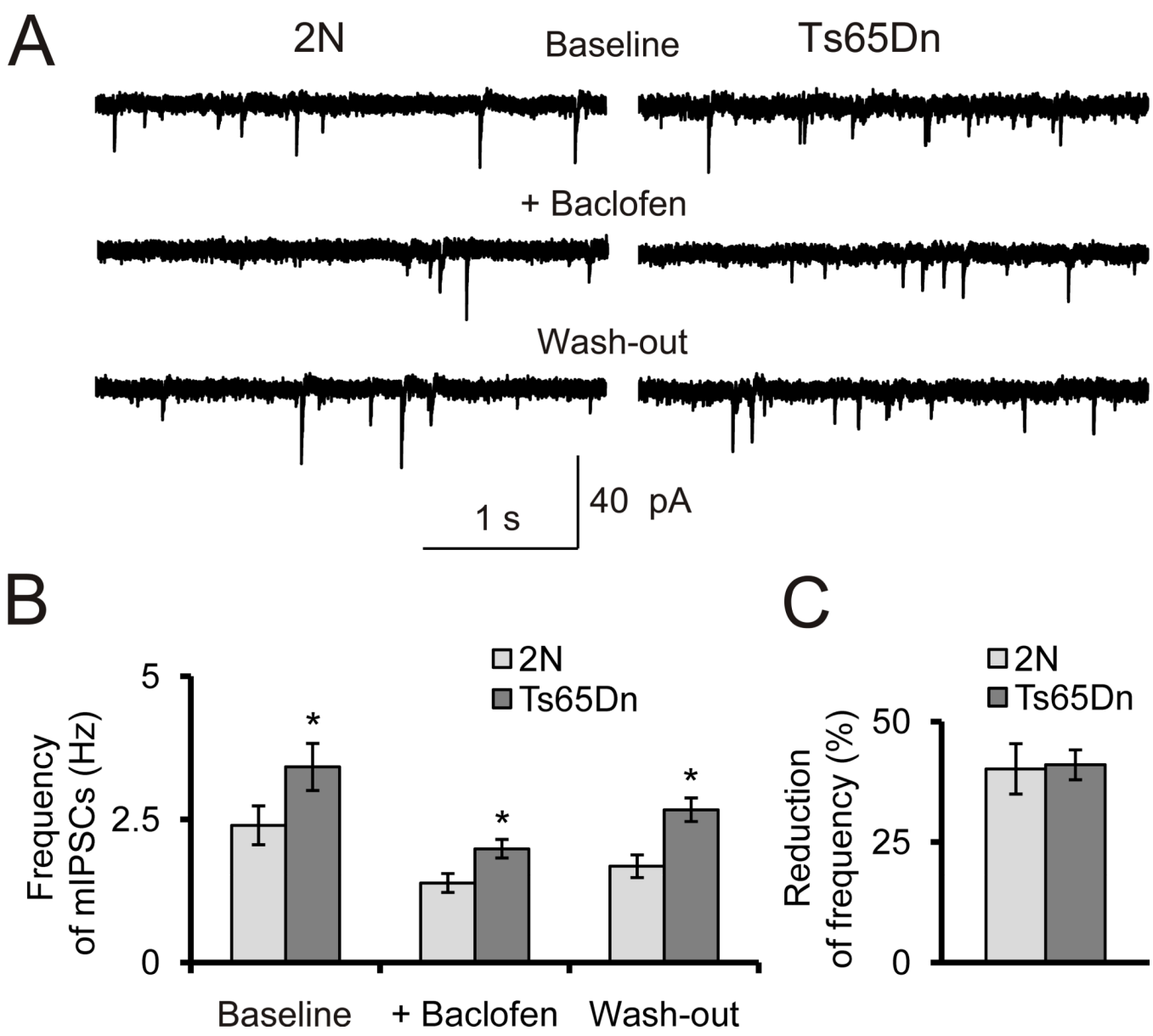


**Figure 4.**

Frequency of mIPSCs was equally affected by the GABAB agonist baclofen (40 μM) in 2N and Ts65Dn granule cells. (A) Examples of spontaneous whole-cell currents in 2N (left) and Ts65Dn (right) cells. (B) Quantification of the data. Baseline frequency of mIPSCs was significantly greater in Ts65Dn cells. Application of baclofen reduced the mIPSC frequency in both 2N and Ts65Dn cells. *$p < 0.03$ for 2N vs. Ts65Dn. (C) Expressed as percents of the baseline values, the reduction of mIPSC frequency was similar in 2N and Ts65Dn cells.

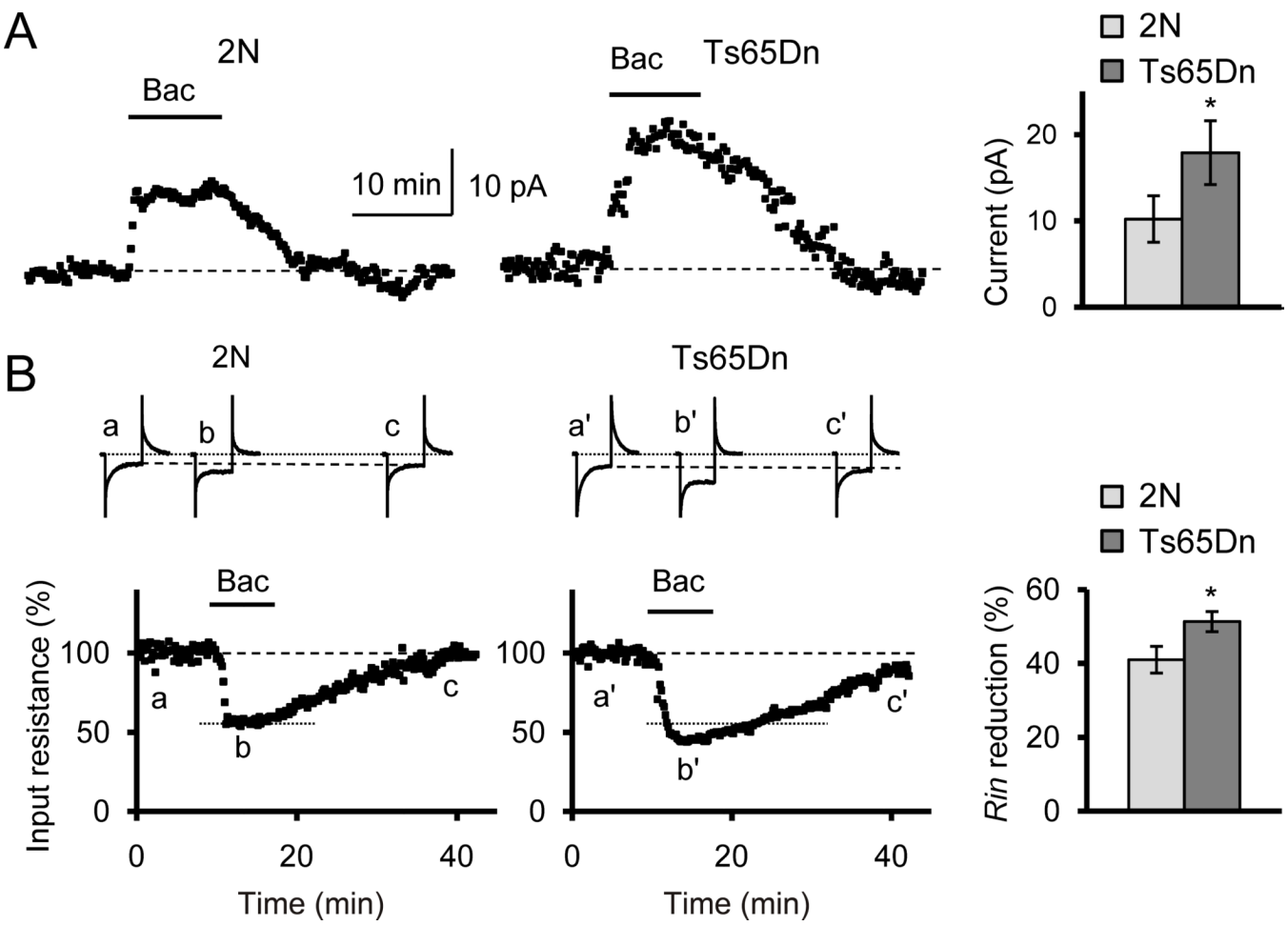


**Figure 5.**

Bath application of the GABAB receptor agonist baclofen had greater postsynaptic effects in Ts65Dn cells. (A) Whole-cell currents evoked by baclofen (40 μM) were greater in Ts65Dn than in 2N cells. Holding potential −80 mV. *$p < 0.05$. (B) Changes of input resistance (*Rin*) during baclofen application were greater in Ts65Dn cells. On top are examples of currents on hyperpolarizing steps (40 ms, 10 mV) that were used to measure the input resistance before (a, a'), during (b, b') and after (c, c') application of baclofen. *$p < 0.03$.

## Table 1

Levels of proteins in the hippocampus of 3-month-old 2N and Ts65Dn mice by Western blot. Numbers of mice for each group are shown in brackets. Mean ± SEM.

| Protein | Band, kDa | 2N | Ts65Dn | p |
|---|---|---|---|---|
| GABAAα1 | 49 | 95.5 ± 4.0 (12) | 84.3 ± 5.3 (10) | 0.09 |
| GABAAα2 | 55 | 93.2 ± 7.8 (12) | 93.3 ± 9.9 (10) | 0.99 |
| GABAAα3 | 56 | 100.2 ± 4.7 (11) | 99.7 ± 7.6 (8) | 0.95 |
| GABAAα5 | 55 | 50.0 ± 1.3 (12) | 45.8 ± 3.1 (10) | 0.17 |
| GABAAγ2 | 48 | 167.6 ± 3.6 (12) | 168.4 ± 6.4(10) | 0.91 |
| GABAB1a | 130 | 36.3 ± 3.4 (5) | 35.3 ± 4.8 (5) | 0.85 |
| GABAB1b | 105 | 80.7 ± 7.4 (5) | 88.9 ± 2.0 (5) | 0.27 |
| Kir3.2 | 43 | **35.0 ± 3.1 (9)** | **55.7 ± 4.3 (9)*** | **<0.001** |
| GAT-1 | 72 | 38.7 ± 2.2 (12) | 41.0 ± 2.9 (10) | 0.49 |
| Actin | 42 | 96.8 ± 4.8 (11) | 95.6 ± 7.9 (8) | 0.88 |

Note a significant increase in the level of Kir3.2 subunits of potassium channels in Ts65Dn samples. Levels the GABAA and GABAB receptor subunits and GABA transporter 1 were not changed.